JOURNAL OF GUIDANCE, CONTROL, AND DYNAMICS
Vol. 43, No. 3, March 2020

Engineering Notes

Finite-Time Concurrent Learning Adaptive Control for Spacecraft with Inertia Parameter Identification

Qin Zhao* and Guangren Duan†
Harbin Institute of Technology, 150001 Harbin, People's Republic of China

https://doi.org/10.2514/1.G004803

I. Introduction

FUTURE space missions will focus on onorbit servicing, such as the removal of space debris and the maintenance of nonfunctional satellites by spacecraft. The inertia properties of the whole system may change significantly after a service spacecraft captures a noncooperative target [1,2]. Furthermore, the attitude and position reference tracking of the combined spacecraft are expected to achieve a rapid and accurate response to various maneuvering commands in the presence of unknown inertia parameters. When designing control systems, however, most of the existing literature deals with parametric uncertainty based on the assumption that the parameters have either known upper and lower bounds or known nominal values. This assumption is strict for noncooperative targets, and the control response cannot be performed optimally with a wide range of parameters or inaccurate nominal values. Hence, it is necessary for spacecraft that the controller has the capability to identify inertia parameters on orbit.

Attempts for online inertia parameter identification have been made with considerable progress. One such identification method uses least squares or other filtering techniques after converting the equations of motion into a linear form in terms of the unknown parameters. The inertia matrix identification for a rigid spacecraft was formulated as a Kalman filter and performed by using double-gimballed control-moment gyroscopes in Ref. [3]. Recursive least-squares-based algorithms are presented in Ref. [4] to identify the inertia matrix by using gyroscope signals. There have also been other solutions that can be referred to as momentum-based methods. In Ref. [5], the inertia parameters are identified based on the linear and angular conservation-of-momentum principle through changing the inertia distribution of the spacecraft system by use of an onboard robotic arm. Angular momentum of the spacecraft was included as part of the estimated state in an extended Kalman filter scheme in Ref. [6] to produce the estimate of inertia parameters, and then the rotational kinetic energy was combined to improve the quality of the estimate. However, once reference tracking is taken into account, not only does a controller need to be designed, but an additional estimator is required when the methods proposed in these references are chosen to identify inertia parameters. This can make the control system complex and computationally intensive.

Received 5 September 2019; revision received 30 October 2019; accepted for publication 30 October 2019; published online 26 November 2019.

*Ph.D. Student, School of Astronautics; zhaoqin129@126.com.
†Professor, School of Astronautics; g.r.duan@hit.edu.cn.

Control-based methods have advantages over the previous ones, which can ensure reference tracking as well as the inertia parameter identification at the same time. It has been well recognized that adaptive control methods can solve the online reference tracking and identification problem under the persistent excitation (PE) condition. For identifying the spacecraft inertia matrix, an adaptive feedback control law was proposed in Ref. [7] by tracking periodic command signals asymptotically. Under the given sufficient condition in Refs. [8,9], mass and inertia matrix identification was addressed through an adaptive tracking controller. A computational adaptive optimal controller was introduced in Ref. [10]. Although there are fruitful results on control-based approaches for inertia parameter identification of spacecraft, the PE condition has to be satisfied for the sufficient richness requirement to ensure the convergence of estimated inertia parameters. Nevertheless, this may lead to unnecessary maneuvering, and thus cause fuel wasting. More recently, a data-based adaptive method, called concurrent learning, was originally proposed in Refs. [11,12] to tackle the "richness" problem that is so common in the field of adaptive control. Instead of the requirement of persistent excitation, this technique uses past and current data concurrently to build a matrix of which the rank is required to be the same as the dimensionality of the uncertainty. It also makes it easy to verify whether the richness condition is met online. This method is subsequently implemented for spacecraft trajectory tracking with identification of mass properties by using the dual quaternion formulation [13]. Asymptotic convergence of reference tracking and parameter identification is finally ensured.

Although spacecraft inertia parameter identification can be realized by using existing adaptive control methods, almost all of the previously discussed control schemes require infinite time to accomplish parameter identification and reference tracking. Obviously, finite-time control techniques are a better option when used to perform some space missions that require higher control accuracy and maneuverability. This Note extends concurrent learning to the field of finite-time control. A finite-time concurrent learning adaptive law is proposed for inertia parameter identification without persistent excitation required. Then, by using backstepping (which is a recursive design technique by considering some state variables as "virtual controls"), a relative translational and rotational controller for the combined spacecraft is designed without a priori information about the mass and inertia matrix. To address the problem of input saturation, an auxiliary system modified from Ref. [14] is introduced. The finite-time convergence of reference tracking and inertia parameter identification is finally guaranteed, and numerical simulations demonstrate the effectiveness of the proposed controller.

II. Spacecraft Model

Consider the combined spacecraft operating in a disturbance-free environment. As shown in Fig. 1, the combined system is composed of a service spacecraft, a manipulator, and a noncooperative target without control capability. It is assumed that the three components are rigid and no relative motion exists between them. Due to the coupling between the translational and rotational motion, even between control force and control torque [15], six-degree-of-freedom (6-DOF) relative coupled dynamics are adopted for the combined spacecraft.

Let $\mathcal{F}_i$ (O-$x_iy_iz_i$) be the Earth-centered inertial frame. Define $\mathcal{F}_p$ (O_p-$x_py_pz_p$) as the body frame of the combined spacecraft, where $\mathcal{F}_p$ is fixed on the center of mass O_p of the combined spacecraft; and O_px_p, O_py_p, and O_pz_p are three mutually perpendicular axes, as shown in Fig. 2. Also, define $\mathcal{F}_t$ (O_t-$x_ty_tz_t$) as the virtual reference body frame, for which the origin and rotation denote the reference position and reference attitude, respectively.

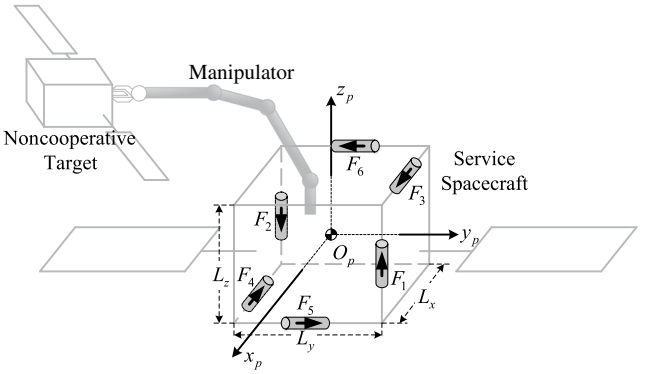

Fig. 1 Illustration of combined spacecraft system and thruster layout.

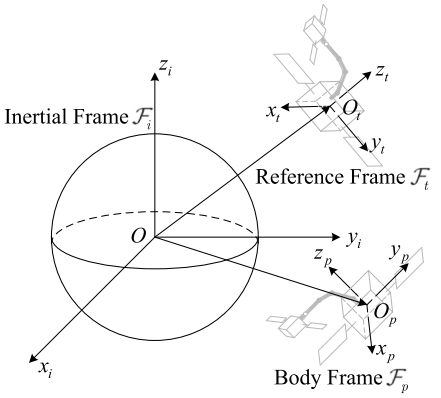

Fig. 2 Coordinate frames.

In the following, $\omega^c_{b,a}$ denotes the angular velocity of $\mathcal{F}_a$ relative to $\mathcal{F}_b$ expressed in $\mathcal{F}_c$, $r^c_{b,a}$ denotes the position of the origin of $\mathcal{F}_a$ relative to that of $\mathcal{F}_b$ expressed in $\mathcal{F}_c$, and R^b_a represents the rotation matrix from $\mathcal{F}_a$ to $\mathcal{F}_b$. Also, $\|\cdot\|$ denotes the Euclidean norm of a vector or the induced norm of a matrix; and $\lambda_{\max}(\cdot)$ and $\lambda_{\min}(\cdot)$ denote the maximum and minimum eigenvalues of $\cdot$, respectively.

A. Relative Attitude Model

The rotation matrix describing rotations from $\mathcal{F}_t$ to $\mathcal{F}_p$ can be represented as

$$R^p_t = I - 4\frac{1-\sigma^T\sigma}{(1+\sigma^T\sigma)^2}S(\sigma) + \frac{8}{(1+\sigma^T\sigma)^2}S^2(\sigma)$$

where σ are the modified Rodrigues parameters, and $S(\sigma) = \sigma\times$ is the cross-product operator.

The relative attitude kinematics of frame $\mathcal{F}_p$ with respect to the reference attitude is given by

$$\dot{\sigma} = G(\sigma)\omega \tag{1}$$

where

$$G(\sigma) = \frac{1}{4}[(1-\sigma^T\sigma)I + 2S(\sigma) + 2\sigma\sigma^T]$$

and $\omega = \omega^p_{i,p} - R^p_t\omega^t_{i,t}$ is the relative angular velocity between $\mathcal{F}_p$ and $\mathcal{F}_t$. Moreover, the relative attitude dynamics can be expressed as [16,17]

$$J\dot{\omega} + C_r\omega + n_r = \tau \tag{2}$$

where τ is the control torque, the inertia matrix of the combined spacecraft is denoted as

$$J = \begin{bmatrix} J_{11} & J_{12} & J_{13} \\ J_{12} & J_{22} & J_{23} \\ J_{13} & J_{23} & J_{33} \end{bmatrix}$$

$$C_r = JS(R^p_t\omega^t_{i,t}) + S(R^p_t\omega^t_{i,t})J - S(J(\omega + R^p_t\omega^t_{i,t}))$$

is an antisymmetric matrix, and

$$n_r = S(R^p_t\omega^t_{i,t})JR^p_t\omega^t_{i,t} + JR^p_t\dot{\omega}^t_{i,t}$$

is a derived nonlinear vector.

B. Relative Translational Model

According to the fundamental equation of the two-body problem with an assumption of small spacecraft mass relative to the Earth [18], the relative translational dynamics described in $\mathcal{F}_p$ can be represented as [19]

$$\dot{p} = v - S(\omega^p_{i,p})p \tag{3}$$

$$m\dot{v} = -mS(\omega^p_{i,p})v - \frac{\mu m}{r_p^3}(p + R^p_t r^t_{i,t}) - mR^p_t\ddot{r}^t_{i,t} + f \tag{4}$$

where $p = r^p_{i,p} - R^p_t r^t_{i,t}$ is the relative position from the desired position to the current position, v is the relative velocity, μ is the Earth's gravitational parameter, m is the mass of the combined spacecraft, r_p is the distance from the center of the Earth to the combined spacecraft, and f is the orbital control force.

C. Thruster Layout

A fully actuated system is employed for both the position and attitude control [20]. As illustrated in Fig. 1, there are six thrusters, and each thruster generates a force of F_i $(i = 1,\ldots,6)$ parallel with the axes of $\mathcal{F}_p$. It is assumed that the thrusters are bidirectional with the positive direction shown in the figure. The control input to the combined spacecraft can be written as

$$u = \begin{bmatrix} f \\ \tau \end{bmatrix} = AF \tag{5}$$

where $F = [F_1 \quad F_2 \quad F_3 \quad F_4 \quad F_5 \quad F_6]^T$ is the thrust input, and A is the input matrix. Assume that the center of mass of the noncooperative target has been estimated in the precapture phase [21,22]. The center of mass of the combined spacecraft can then be obtained by combining with the known inertia properties of the service spacecraft. For simplicity, the center of mass of the combined spacecraft is set at the geometric center of the service spacecraft. Hence, with the dimensions L_x, L_y, and L_z of the service spacecraft, A can be given by

$$A = \begin{bmatrix} 0 & 0 & 1 & -1 & 0 & 0 \\ 0 & 0 & 0 & 0 & 1 & -1 \\ 1 & -1 & 0 & 0 & 0 & 0 \\ \frac{L_y}{2} & \frac{L_y}{2} & 0 & 0 & \frac{L_z}{2} & \frac{L_z}{2} \\ -\frac{L_x}{2} & -\frac{L_x}{2} & \frac{L_z}{2} & \frac{L_z}{2} & 0 & 0 \\ 0 & 0 & -\frac{L_y}{2} & -\frac{L_y}{2} & \frac{L_x}{2} & \frac{L_x}{2} \end{bmatrix} \tag{6}$$

Furthermore, due to the physical limitation, the thrust input is subject to saturation nonlinearity described by

$$F = \mathrm{Sat}(F_{\mathrm{in}}) \tag{7}$$

where $F_{\text{in}} = [\, F_{\text{in},1} \quad \cdots \quad F_{\text{in},6} \,]^T$ is the actual thrust input signal, and $\text{Sat}(F_{\text{in}}) = [\, \text{sat}(F_{\text{in},1}) \quad \cdots \quad \text{sat}(F_{\text{in},6}) \,]^T$. Here, $\text{sat}(\cdot)$ denotes the saturation function defined as

$$\text{sat}(F_{\text{in},i}) = \begin{cases} F_{\max}, & \text{if } F_{\text{in},i} > F_{\max} \\ F_{\text{in},i}, & \text{if } F_{\min} \le F_{\text{in},i} \le F_{\max} \\ F_{\min}, & \text{if } F_{\text{in},i} < F_{\min} \end{cases}$$

where $F_{\max}$ and $F_{\min}$ are the upper and lower limits, respectively.

D. Six-Degree-of-Freedom Integrated Model

To obtain the 6-DOF integrated model of relative translational and attitude motion for the combined spacecraft, define the state vectors $x_1 = [\, p^T \quad \sigma^T \,]^T$ and $x_2 = [\, v^T \quad \omega^T \,]^T$. Based on Eqs. (1–5), the relative coupled dynamics can be written in the following compact form:

$$\dot{x}_1 = C_1 x_1 + \Lambda x_2 \tag{8}$$

$$M\dot{x}_2 = -C_2 x_2 - n + AF \tag{9}$$

where

$$\Lambda = \begin{bmatrix} I & 0_{3\times3} \\ 0_{3\times3} & G(\sigma) \end{bmatrix} \in \mathbb{R}^{6\times6},$$

$$C_1 = \begin{bmatrix} -S(R_t^p \omega_{i,t}^t) & 0_{3\times3} \\ 0_{3\times3} & 0_{3\times3} \end{bmatrix} \in \mathbb{R}^{6\times6},$$

$$C_2 = \begin{bmatrix} mS(\omega_{i,p}^p) & 0_{3\times3} \\ 0_{3\times3} & C_r \end{bmatrix} \in \mathbb{R}^{6\times6},$$

$$M = \begin{bmatrix} mI_3 & 0_{3\times3} \\ 0_{3\times3} & J \end{bmatrix} \in \mathbb{R}^{6\times6},$$

$$n = \begin{bmatrix} \frac{\mu m}{r_p^3}(p + R_t^p r_{i,t}^t) + mR_t^p \ddot{r}_{i,t}^t \\ n_r \end{bmatrix} \in \mathbb{R}^6$$

III. Adaptive Finite-Time Control with Parameter Identification

The control objective is to identify the mass and inertia matrix of the combined spacecraft in finite time by extending the results proposed in Ref. [12] while the combined spacecraft tracks a reference trajectory at the same time. Before giving the main results, the fol lowing definition and assumptions are given:

Definition 1 [23]: Consider the nonlinear system $\dot{x} = f(x, u)$, where x is a state vector and u is the input vector. The solution is practical finite-time stable (PFS) if, for all $x(t_0) = x_0$, there exist $\xi > 0$ and $T(\xi, x_0) < \infty$ such that $\|x(t)\| < \xi$ for all $t \ge t_0 + T$.

Assumption 1: The linear acceleration $\dot{v}$ and angular acceleration $\dot{\omega}$ can be known through explicit measurements or estimators such as a fixed-point smoother.

Assumption 2: The desired trajectories $r_{i,t}^t$, $\dot{r}_{i,t}^t$, $\omega_{i,t}^t$, and $\dot{\omega}_{i,t}^t$ are smooth, bounded, and known.

A. Finite-Time Concurrent Learning Parameter Identification

Define a linear operator $L{:}\mathbb{R}^3 \to \mathbb{R}^{3\times6}$ as

$$L(a) = \begin{bmatrix} a_1 & 0 & 0 & 0 & a_3 & a_2 \\ 0 & a_2 & 0 & a_3 & 0 & a_1 \\ 0 & 0 & a_3 & a_2 & a_1 & 0 \end{bmatrix}$$

for arbitrary $a = [\, a_1 \quad a_2 \quad a_3 \,]^T \in \mathbb{R}^3$.

Therefore, the two terms $S(R_t^p \omega_{i,t}^t) J R_t^p \omega_{i,t}^t$ and $J R_t^p \dot{\omega}_{i,t}^t$ in the nonlinear vector n of Eq. (9) can be rewritten in the following parametric expressions:

$$S(R_t^p \omega_{i,t}^t) J R_t^p \omega_{i,t}^t = S(R_t^p \omega_{i,t}^t) L(R_t^p \omega_{i,t}^t)\theta_J, \; J R_t^p \dot{\omega}_{i,t}^t = L(R_t^p \dot{\omega}_{i,t}^t)\theta_J$$

where $\theta_J = [\, J_{11} \quad J_{22} \quad J_{33} \quad J_{23} \quad J_{13} \quad J_{12} \,]^T$.

For identifying m together with the elements of J, let $\theta = [\, m \quad \theta_J^T \,]^T$; then, n can be transformed into the following form:

$$n = N_1 \theta \tag{10}$$

where

$$N_1 = \begin{bmatrix} \frac{\mu}{r_p^3}(p + R_t^p r_{i,t}^t) + R_t^p \ddot{r}_{i,t}^t & 0_{3\times6} \\ 0_{3\times1} & S(R_t^p \omega_{i,t}^t) L(R_t^p \omega_{i,t}^t) + L(R_t^p \dot{\omega}_{i,t}^t) \end{bmatrix}$$

In a similar way, the following relationships hold:

$$M\dot{x}_2 = N_2 \theta, \qquad C_2 x_2 = N_3 \theta \tag{11}$$

where

$$N_2 = \begin{bmatrix} \dot{v} & 0_{3\times6} \\ 0_{3\times1} & L(\dot{\omega}) \end{bmatrix}, \qquad N_3 = \begin{bmatrix} S(\omega_{i,p}^p) v & 0_{3\times6} \\ 0_{3\times1} & N_{3,22} \end{bmatrix}$$

with

$$N_{3,22} = L(S(R_t^p \omega_{i,t}^t)\omega) + S(R_t^p \omega_{i,t}^t) L(\omega) + S(\omega) L(\omega + R_t^p \omega_{i,t}^t)$$

Then, Eq. (9) can be rewritten as

$$\Phi(x)\theta = AF \tag{12}$$

where $\Phi(x) = N_1 + N_2 + N_3$ is termed as a regressor matrix.

To meet the richness condition as mentioned in the Introduction (Sec. I), some data need to be recorded. Let $j \in \{1, 2, \ldots, q\}$ denote the index of a stored data point x_j, where q denotes the subscript of the last point stored. Let $\Phi(x_j)$ and F_j denote the evaluated regressor matrix and thrust input, respectively, at point x_j. Let $\hat{\theta}$ denote the estimate of θ. Define $\epsilon_j = \Phi(x_j)\tilde{\theta}$, where $\tilde{\theta} = \theta - \hat{\theta}$ is the parameter estimation error. Then, it follows from Eq. (12) that

$$\epsilon_j = AF_j - \Phi(x_j)\hat{\theta}$$

Using the following criteria to select the instantaneous data $\Phi(x)$ [24],

$$\frac{\|\Phi(x) - \Phi(x_q)\|^2}{\|\Phi(x)\|} \ge \kappa$$

store $\Phi(x)$ and corresponding F in history stacks Φ_{st} and F_{st}, respectively, in a cyclical manner, where κ is a positive scalar. The maximum allowable number of recorded points is $\bar{q} \ge q$. To guarantee the sufficient richness of the recorded data, the following condition is presented.

Condition 1: The recorded data are sufficiently rich such that the sum of the recorded $\Phi^T(x_j)\Phi(x_j)$ is of full rank. That is, if

$$\Omega = \sum_{j=1}^{q} \Phi^T(x_j)\Phi(x_j)$$

then $\text{rank}(\Omega) = 7$.

Design the concurrent learning adaptive law for $\hat{\theta}$ as

$$\dot{\hat{\theta}} = \Gamma \frac{\sum_{j=1}^{q} \Phi^T(x_j)\epsilon_j}{\| \sum_{j=1}^{q} \Phi^T(x_j)\epsilon_j \|} \tag{13}$$

where Γ is a positive definite gain matrix. Then, the following theorem holds:

Theorem 1: Consider the system described by Eq. (8) and (9) with the adaptive law [Eq. (13)] and Condition 1; then, the parameter estimation error $\tilde{\theta}$ converges to zero in finite time T_1 bounded by $T_1 \le 2\sqrt{V_1(0)}/\mu_1$.

Proof: Please refer to Appendix A.

B. Control Law Design

In this subsection, combining with the concurrent learning adaptive law proposed in Eq. (13), a finite-time control law is designed for the combined spacecraft to achieve trajectory tracking and parameter identification, where Condition 1 is still required to be satisfied.

Design the following virtual control as an intermediate control law:

$$\alpha = -\left(K_1 + \frac{1}{4\gamma^2} I\right)\Lambda^T x_1 - \Lambda^{-1} K_2 \frac{x_1}{\|x_1\|} \tag{14}$$

where K_1 and K_2 are positive definite matrices, and γ is a positive scalar. To simplify the determination of the derivative of α, let α pass through the following first-order filter:

$$\tau_c \dot{\alpha}_c + \alpha_c = \alpha \tag{15}$$

where α_c is the filtered version of α, and $\tau_c > 0$ is the filter time constant. The filter error is denoted as $e_\alpha = \alpha_c - \alpha$.

Define

$$\tilde{x}_2 = x_2 - \alpha_c \tag{16}$$

Then, it follows that

$$\tilde{x}_2 = x_2 - \alpha - e_\alpha \tag{17}$$

Consider the Lyapunov function candidate

$$V_2 = \frac{1}{2} x_1^T x_1 \tag{18}$$

Invoking Eq. (8), the time derivative of V_2 is given by

$$\dot{V}_2 = x_1^T C_1 x_1 + x_1^T \Lambda(\tilde{x}_2 + \alpha + e_\alpha) \tag{19}$$

Noticing $x_1^T C_1 x_1 = 0$ and substituting Eq. (14) into Eq. (19), we have

$$\dot{V}_2 = -x_1^T \Lambda\left(K_1 + \frac{1}{4\gamma^2} I\right)\Lambda^T x_1 - x_1^T K_2 \frac{x_1}{\|x_1\|} + x_1^T \Lambda \tilde{x}_2 + x_1^T \Lambda e_\alpha \tag{20}$$

On the other hand, by combining with Eq. (16), Eq. (9) can be rewritten as

$$M\dot{\tilde{x}}_2 = -C_2\tilde{x}_2 - C_2\alpha_c - n - M\dot{\alpha}_c + AF \tag{21}$$

Using the similar transformation method to Eq. (11) yields

$$M\dot{\alpha}_c = N_{2'}\theta, \qquad C_2\alpha_c = N_{3'}\theta$$

where $N_{2'}$ and $N_{2'}$ are obtained from N_2 and N_3 by replacing $\dot{x}_2$ and x_2 with $\dot{\alpha}_c$ and α_c, respectively. Hence, Eq. (9) can also be written as

$$M\dot{\tilde{x}}_2 = -C_2\tilde{x}_2 - N\theta + AF \tag{22}$$

where $N = N_1 + N_{2'} + N_{3'}$.

To analyze the input saturation conveniently, an auxiliary system is introduced [14]:

$$\dot{x}_a = \begin{cases} -k_{a_1}\dfrac{x_a}{\|x_a\|} - k_{a_2}x_a - \dfrac{g(\Delta F)}{\|x_a\|^2}x_a - A\Delta F, & \|x_a\| \ge \eta \\ 0, & \|x_a\| < \eta \end{cases} \tag{23}$$

where x_a is the state of the auxiliary system; k_{a_1}, k_{a_2}, and η are positive scalars; $\Delta F = F - F_{\text{in}}$; and $g(\Delta F) = \|A\|^2\|\Delta F\|^2$. When $\|x_a\| \ge \eta$ holds, there exists input saturation, whereas $\|x_a\| < \eta$ means that there is no input saturation.

Consider the situation where the input saturation exists. Choose the following Lyapunov function candidate:

$$V_3 = V_2 + \frac{1}{2}\tilde{x}_2^T M\tilde{x}_2 + \frac{1}{2}\tilde{\theta}^T\Gamma^{-1}\tilde{\theta} + \frac{1}{2}x_a^T x_a \tag{24}$$

where Γ is a positive definite matrix. Combining with Eqs. (20), (22), and (23), the time derivative of V_3 is given by

$$\begin{aligned}\dot{V}_3 = {} & -x_1^T\Lambda\left(K_1 + \frac{1}{4\gamma^2} I\right)\Lambda^T x_1 - x_1^T K_2 \frac{x_1}{\|x_1\|} + x_1^T\Lambda\tilde{x}_2 + x_1^T\Lambda e_\alpha \\ & + \tilde{x}_2^T(-C_2\tilde{x}_2 - N\theta + AF) - \tilde{\theta}^T\Gamma^{-1}\dot{\hat{\theta}} - k_{a_1}\|x_a\| - k_{a_2}\|x_a\|^2 \\ & - g(\Delta F) - x_a^T A\Delta F \end{aligned} \tag{25}$$

Design the actual thrust input signal as

$$F_{\text{in}} = A^{-1}\left(N\hat{\theta} - \Lambda^T x_1 - K_3\tilde{x}_2 - K_4\frac{\tilde{x}_2}{\|\tilde{x}_2\|} - K_5 x_a\right) \tag{26}$$

and the concurrent learning adaptive law as

$$\dot{\hat{\theta}} = \Gamma\left[-N^T\tilde{x}_2 + \frac{K_6\sum_{j=1}^{q}\Phi^T(x_j)\epsilon_j}{\|\sum_{j=1}^{q}\Phi^T(x_j)\epsilon_j\|}\right] \tag{27}$$

where K_3, K_4, K_5, and K_6 are positive definite gain matrices.

Noticing $\tilde{x}_2^T C_2\tilde{x}_2 = 0$ and substituting Eqs. (26) and (27) into Eq. (25), we have

$$\begin{aligned}\dot{V}_3 = {} & -x_1^T\Lambda\left(K_1 + \frac{1}{4\gamma^2} I\right)\Lambda^T x_1 - x_1^T K_2\frac{x_1}{\|x_1\|} + x_1^T\Lambda e_\alpha - \tilde{x}_2^T K_3\tilde{x}_2 \\ & - \tilde{x}_2^T K_4\frac{\tilde{x}_2}{\|\tilde{x}_2\|} - \tilde{\theta}^T\frac{K_6\sum_{j=1}^{q}\Phi^T(x_j)\epsilon_j}{\|\sum_{j=1}^{q}\Phi^T(x_j)\epsilon_j\|} - k_{a_1}\|x_a\| - k_{a_2}\|x_a\|^2 \\ & - g(\Delta F) - x_a^T A\Delta F + \tilde{x}_2^T A\Delta F - \tilde{x}_2^T K_5 x_a \end{aligned}$$

Employing the following equation

$$-\frac{1}{4\gamma^2}x_1^T\Lambda\Lambda^T x_1 + x_1^T\Lambda e_\alpha = \gamma^2 e_\alpha^T e_\alpha - \gamma^2\left\|e_\alpha - \frac{1}{2\gamma^2}\Lambda^T x_1\right\|^2$$

and inequalities

$$\begin{aligned} -x_a^T A\Delta F &\le \frac{1}{2}\|x_a\|^2 + \frac{1}{2}\|A\|^2\|\Delta F\|^2 \\ \tilde{x}_2^T A\Delta F &\le \frac{1}{2}\|\tilde{x}_2\|^2 + \frac{1}{2}\|A\|^2\|\Delta F\|^2 \\ -\tilde{x}_2^T K_5 x_a &\le \frac{1}{2}\|\tilde{x}_2\|^2 + \frac{1}{2}\|K_5\|^2\|x_a\|^2 \end{aligned}$$

the derivative of V_3 is finally derived as

$$\dot{V}_3 \le -x_1^T \Lambda K_1 \Lambda^T x_1 - x_1^T K_2 \frac{x_1}{\|x_1\|} - (\lambda_{\min}(K_3) - 1)\|\tilde{x}_2\|^2 - \tilde{x}_2^T K_4 \frac{\tilde{x}_2}{\|\tilde{x}_2\|} - \tilde{\theta}^T \frac{K_6 \Omega \tilde{\theta}}{\|\Omega \tilde{\theta}\|} + \gamma^2 e_\alpha^T e_\alpha - \gamma^2 \left\| e_\alpha - \frac{1}{2\gamma^2} \Lambda^T x_1 \right\|^2 - k_{a_1}\|x_a\| - \left(k_{a_2} - \frac{1}{2}\lambda_{\max}^2(K_5) - \frac{1}{2} \right)\|x_a\|^2$$

If the control gains satisfy,

$$\lambda_{\min}(K_3) - 1 > 0, \qquad k_{a_2} - \frac{1}{2}\lambda_{\max}^2(K_5) - \frac{1}{2} > 0 \tag{28}$$

yields

$$\dot{V}_3 \le -\lambda_{\min}(K_2)\|x_1\| - \lambda_{\min}(K_4)\|x_2\| - \lambda_{\min}(K_6\Omega)/\lambda_{\max}(\Omega)\|\tilde{\theta}\| - \lambda_{\min}(k_{a_1})\|x_a\| + \gamma^2 e_\alpha^T e_\alpha \tag{29}$$

The preceding design procedure can be summarized in the following theorem, which contains the results of the adaptive control for the combined spacecraft in the presence of unknown inertia properties and input saturation.

Theorem 2: Consider the system described by Eqs. (8) and (9) with Condition 1 satisfied. If the actual thrust input signal is designed as Eq. (26) with the chosen control gains satisfying Eq. (28), and the estimation $\hat{\theta}$ is updated by Eq. (27), then the closed-loop system is PFS; that is, the tracking errors x_1 and x_2 as well as the estimation error $\tilde{\theta}$ converge to a neighborhood of the origin in finite time T^*, which is given in the proof.

Proof: Please refer to Appendix B.

Remark 1: The input matrix A in Eq. (26) is invertible because A given by Eq. (6) is full of rank.

Remark 2: Because θ cannot be exactly known, the time T^* cannot be prescribed in advance where $\tilde{\theta}$ is involved. Therefore, the theorem can just give the time T^* in theory and guarantee the finite-time convergence of reference tracking and inertia parameter identification.

Remark 3: The gain matrices K_1 to K_6, which affect the convergence speed and precision of the tracking and estimation errors, are required to be positive definite with the inequalities in Eq. (28) satisfied. Large K_1 to K_4 and K_6 will increase the convergence speed but lead to input saturation, and large K_5 will result in large convergence errors. The convergence time also partly depends on the maximum and minimum eigenvalues of Ω; that is, larger $\lambda_{\min}(\Omega)/\lambda_{\max}(\Omega)$ will render a shorter convergence time. Here, the matrix Ω is discrete based on the recorded data. For a continuous implementation of concurrent learning, the reader is referred to Ref. [25], which uses integration instead of summation.

Remark 4: The proposed controller depends on perfect knowledge of the position and attitude information, i.e., p, v, $\dot{v}$, σ, ω, and $\dot{\omega}$, as well as the thrust input F. Hence, the measurement noise and external disturbance can have a potential impact on the convergence performance. Fortunately, the spacecraft system is robust to a certain class of uncertainty, which will be illustrated in the numerical simulations.

Remark 5: To eliminate undesirable chattering, a boundary layer is introduced to smooth the control [26]:

$$\frac{a}{\|a\|} = \begin{cases} \dfrac{a}{\|a\|}, & \text{if } \|a\| > \delta \\ \dfrac{a}{\delta}, & \text{if } \|a\| \le \delta \end{cases} \tag{30}$$

where $\delta > 0$ is the thickness of the boundary layer. As δ approaches zero, the approximate control law can be made arbitrarily close to the original one.

IV. Numerical Simulations

In this section, a 6-DOF combined spacecraft described by Eqs. (8) and (9) is considered. The objective of the simulations is to regulate the spacecraft operating in a circular orbit and maintaining Earth orientation.

To demonstrate the superiority of the proposed finite-time concurrent learning adaptive controller (FTCLAC), we compare the controller with a concurrent learning adaptive controller (CLAC). For the same combined spacecraft system, the update law of the CLAC is

$$\dot{\hat{\theta}} = \Gamma\left[-N^T \tilde{x}_2 + K_6 \sum_{j=1}^{q} \Phi^T(x_j)\epsilon_j \right]$$

according to Ref. [12], and the CLAC has the same virtual control α and actual thrust input signal F_{in} with FTCLAC in Eqs. (14) and (26). In addition, another simulation, termed as FTCLAC(R), with measurement noise and external disturbance is conducted to examine the robustness of the FTCLAC. All the simulation parameters of the FTCLAC, CLAC, and FTCLAC(R) are the same.

Assume that the orbit radius is $r_t = 6628$ km. The Earth's gravitational parameter is $\mu = 3.986 \times 10^{14}$ m^3/s^2, and the orbital angular velocity is $\omega_0 = \sqrt{\mu/r_t^3}$. Therefore, the desired angular velocity is

$$\omega_{i,t}^t = [0 \quad 0 \quad \omega_0]^T, \qquad \dot{\omega}_{i,t}^t = [0 \quad 0 \quad 0]^T$$

Accordingly, the desired attitude of the combined spacecraft can be obtained from

$$\dot{\sigma}_{i,t}^t = G(\sigma_{i,t}^t)\omega_{i,t}^t$$

with the initial value

$$\sigma_{i,t}^t = [0 \quad 0 \quad 0]^T$$

The reference position signals are represented as

$$r_{i,t}^t = [r_t \quad 0 \quad 0]^T, \qquad \ddot{r}_{i,t}^t = -\frac{\mu}{r_t^3} r_{i,t}^t$$

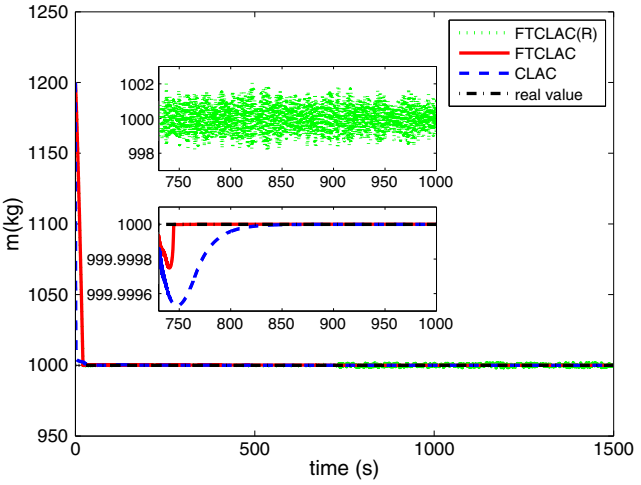

Fig. 3 Estimation of m.

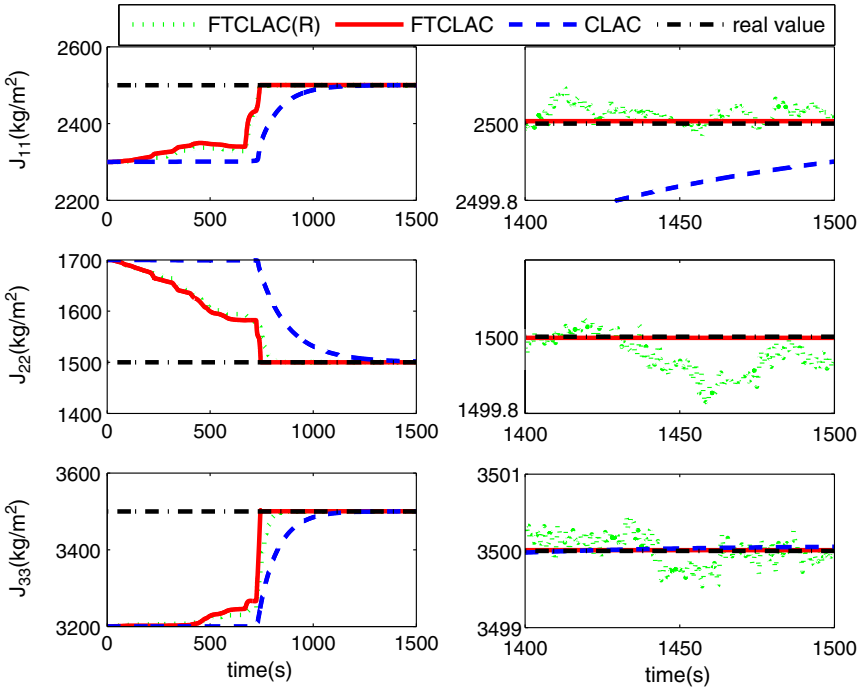

Fig. 4 Estimation of J_{11}, J_{22}, and J_{33}.

The mass of the combined spacecraft is $m = 1000$ kg, the dimensions are $L_x = L_y = L_z = 4$ m, and the inertia matrix is

$$J = \begin{bmatrix} 2500 & 50 & 30 \\ 50 & 1500 & 40 \\ 30 & 40 & 3500 \end{bmatrix} \text{kg} \cdot \text{m}^2$$

The measurements of p, v, σ, and ω are tainted by additive noise assumed as $0.001 \times \text{rand}(3,1)$ m, $2 \times 10^{-5} \times \text{rand}(3,1)$ m/s, $8 \times 10^{-5} \times \text{rand}(3,1)$, and $5 \times 10^{-6} \times \text{rand}(3,1)$ rad/s, respectively. The external disturbance force and torque are set as

$$f_d = \begin{bmatrix} 0.08 - 0.05\sin(\omega_0 t) + 0.02\cos(\omega_0 t) \\ -0.1 + 0.05\sin(\omega_0 t) - 0.01\cos(\omega_0 t) \\ 0.1 + 0.07\sin(\omega_0 t) - 0.03\cos(\omega_0 t) \end{bmatrix} \text{N},$$

$$\tau_d = \begin{bmatrix} 0.01 - 0.008\sin(\omega_0 t) + 0.003\cos(\omega_0 t) \\ 0.008 - 0.006\sin(\omega_0 t) - 0.002\cos(\omega_0 t) \\ 0.01 + 0.005\sin(\omega_0 t) + 0.001\cos(\omega_0 t) \end{bmatrix} \text{N} \cdot \text{m}$$

The initial relative position, relative velocity, relative attitude, relative angular velocity, and the initial estimated parameter are given, respectively, by

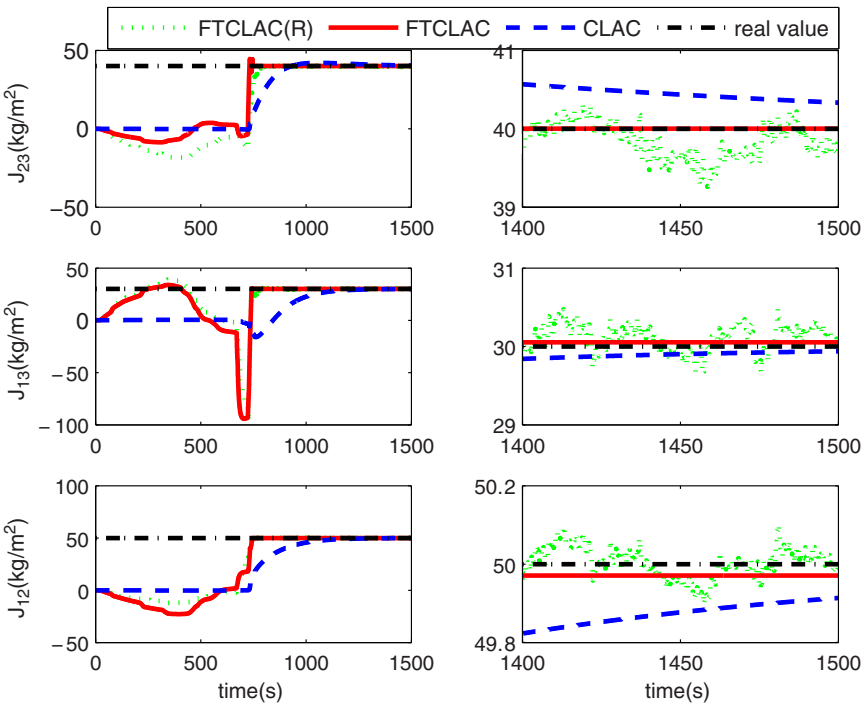

Fig. 5 Estimation of J_{23}, J_{13}, and J_{12}.

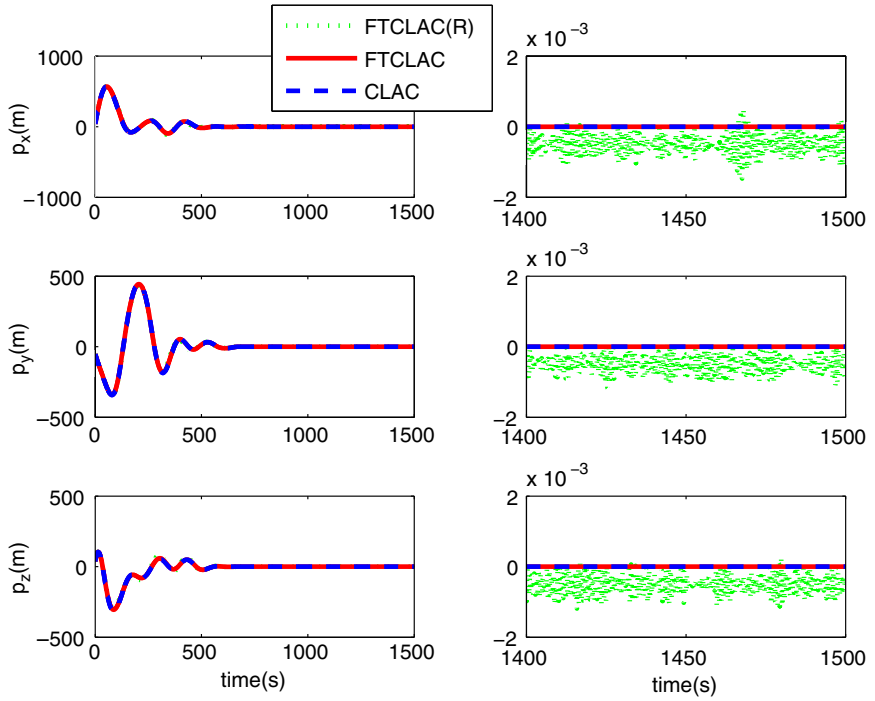

Fig. 6 Response of relative position p.

$$p(0) = [\,30 \quad -50 \quad 35\,]^T \text{ m},$$
$$v(0) = [\,15 \quad -5 \quad 10\,]^T \text{ m/s},$$
$$\sigma(0) = [\,-0.3143 \quad 0.4528 \quad 0.3473\,]^T,$$
$$\omega(0) = [\,0.01 \quad -0.02 \quad 0.01\,]^T \text{ rad/s},$$
$$\hat{\theta}(0) = [\,1200 \quad 2300 \quad 1700 \quad 3200 \quad 0 \quad 0 \quad 0\,]^T$$

The controller gains, filter, and auxiliary system parameters are chosen by trial as $K_1 = 0.012I_{6\times6}$, $\gamma = 30$, $K_2 = \text{diag}\{0.14I_{3\times3}, 8.75\times10^{-3}I_{3\times3}\}$, $K_3 = 1.51I_{6\times6}$, $K_4 = I_{6\times6}$, $K_5 = 0.1I_{6\times6}$, $K_6 = 10I_{7\times7}$, $\Gamma = 1.5I_{7\times7}$, $\tau_c = 2.3$, $k_{a_1} = 1$, and $k_{a_2} = 10$. The initial value of α_c is set as zero. The maximum allowable number of recorded points is $\bar{q} = 15$, and $\kappa = 0.05$. The thickness of the boundary layers for virtual control, the actual thrust input signal, and the adaptive law are, respectively, set as 0.00001, 0.001, and 0.0001. The lower and upper limits of the force generated by thrusters are $F_{\min} = -100$ N and $F_{\max} = 100$ N, respectively.

The identification results of the mass and inertia matrix are illustrated in Figs. 3–5. It is clear that m and J both converge to their real values using the FTCLAC and CLAC in the absence of the persistent excitation condition following the satisfaction of Condition 1. Compared with the asymptotic convergence by using the CLAC, the proposed FTCLAC can also guarantee the finite-time convergence of the mass and inertia matrix with no a priori knowledge required.

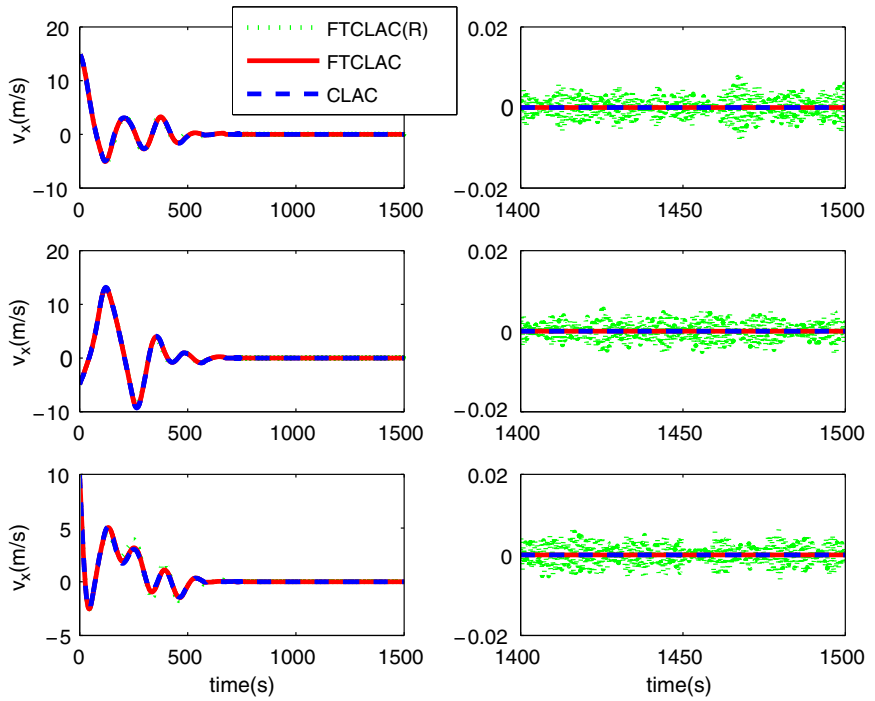

Fig. 7 Response of relative velocity v.

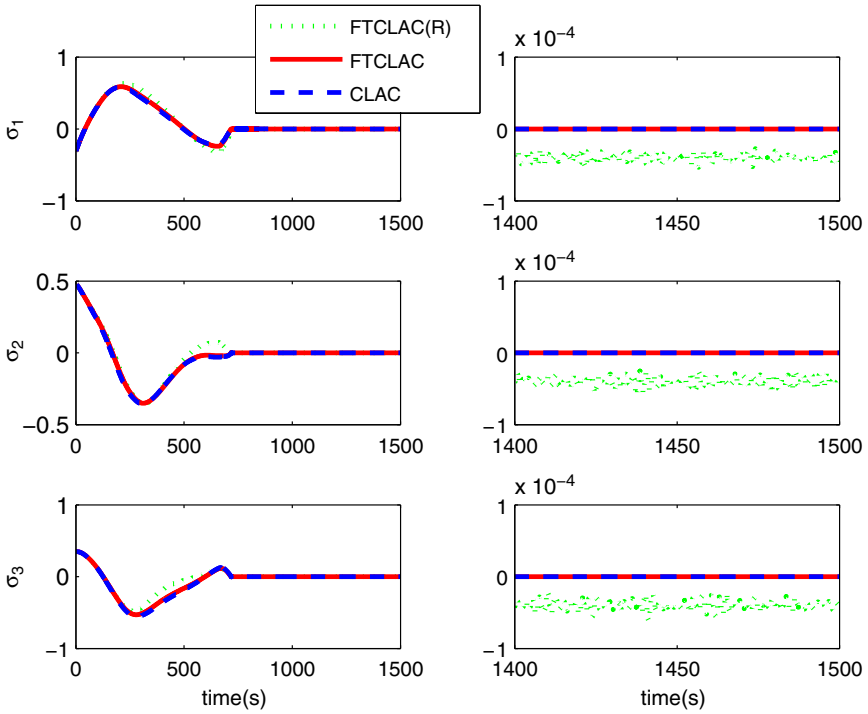

Fig. 8 Response of relative attitude σ.

However, when the measurement noise and external disturbance are taken into account, the estimation errors of inertia parameters are larger than those without these uncertainties, as can be seen from the enlarged parts in Figs. 3–5.

In Figs. 6 and 7, the relative position converges to zero, which means that the combined spacecraft tracks the desired position well and the relative velocity goes to zero without relative translational motion for both the FTCLAC and CLAC. At the same time, as shown in Figs. 8 and 9, the attitude of the combined spacecraft is synchronized with the desired attitude accurately; meanwhile, the relative angular velocity converges to zero. In addition, from the enlarged parts on the right in Figs. 6–9, the tracking errors of the FTCLAC(R) are increased as compared with the FTCLAC due to the measurement noise and external disturbance. In spite of this, the combined spacecraft can still track the reference trajectories, which also turns out the robustness of the proposed controller.

Finally, Fig. 10 illustrates the control force generated by the thrusters for both the FTCLAC and CLAC. It can be seen that all the forces are within 100 N. During the initial phase, there exists input saturation in order to drive the combined spacecraft to the reference trajectories and identify the inertia properties. After that, the forces are almost zero just to maintain Earth orientation.

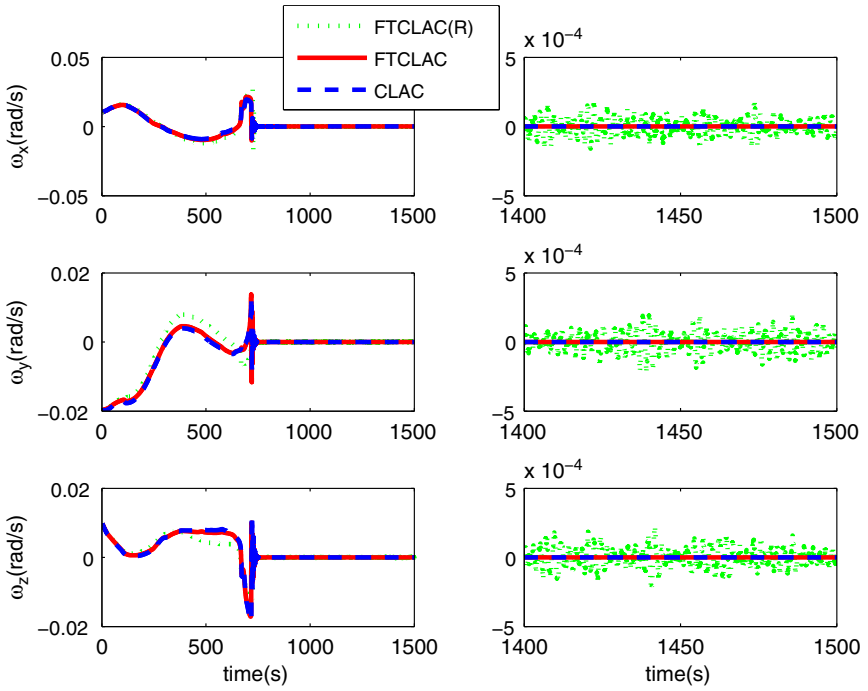

Fig. 9 Response of relative angular velocity ω.

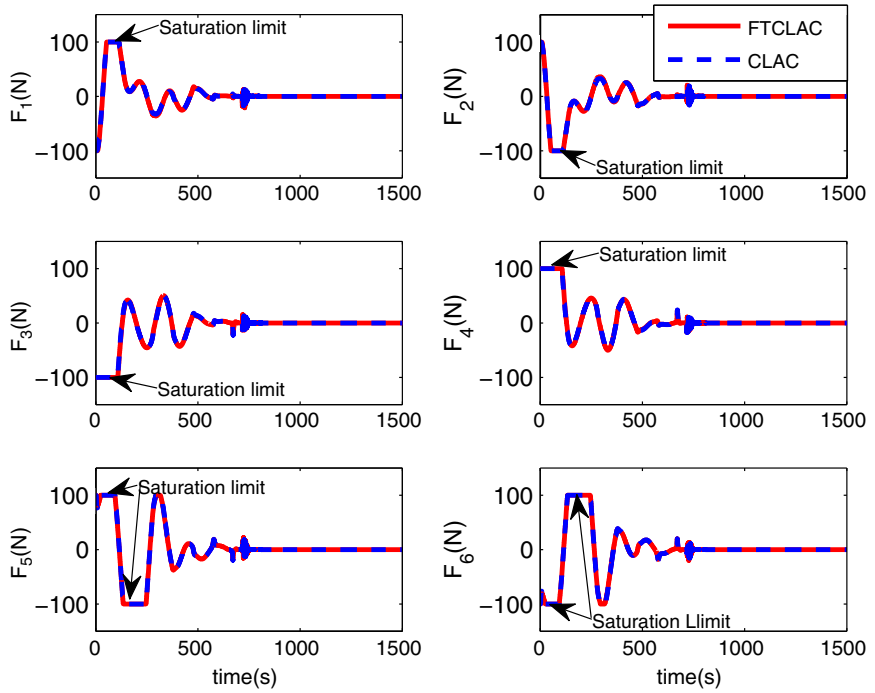

Fig. 10 Response of thrust F.

V. Conclusions

In this Note, a postcapture control problem caused by the change of inertia properties is addressed for the combined spacecraft. Considering the coupling between the translational and rotational motion, 6-DOF relative coupled dynamics are adopted. By extending the existing results, a finite-time concurrent learning adaptive law is proposed for the combined spacecraft based on recorded data without requiring persistent excitation. The sufficient condition to identity the mass and inertia matrix is also given. Furthermore, an integrated controller is designed to achieve reference tracking and inertia parameter identification. The controller requires no a priori knowledge of the mass and inertia matrix of the combined spacecraft and takes the input saturation into account. Simulation results demonstrate not only the effectiveness of the proposed controller but also the robustness against measurement noise and external disturbance.

Appendix A: Proof of Theorem 1

Proof: Choose a candidate Lyapunov function as follows:

$$V_1 = \frac{1}{2}\tilde{\theta}^T\Gamma^{-1}\tilde{\theta}$$

Differentiating V_1 with respect to time and noticing that Ω is positive definite with Condition 1 satisfied yields

$$\begin{aligned}\dot{V}_1 &= -\tilde{\theta}^T\Gamma^{-1}\dot{\hat{\theta}}\\ &= -\tilde{\theta}^T\frac{\sum_{j=1}^{q}\Phi^T(x_j)\epsilon_j}{\|\sum_{j=1}^{q}\Phi^T(x_j)\epsilon_j\|}\\ &= -\tilde{\theta}^T\frac{\Omega\tilde{\theta}}{\|\Omega\tilde{\theta}\|}\\ &\le -\mu_1\sqrt{V_1}\end{aligned}$$

where $\mu_1 = \sqrt{2}\lambda_{\min}(\Omega)/[\lambda_{\max}(\Omega)\sqrt{\lambda_{\max}(\Gamma^{-1})}]$. According to the theorem in Ref. [27], the estimation error $\tilde{\theta}$ converges to zero within $T_1 \le 2\sqrt{V_1(0)}/\mu_1$.

Appendix B: Proof of Theorem 2

Proof: We take Assumption 2, the physical limitation of the thrusters, and the filter defined in Eq. (15) into consideration. According to Ref. [28], there exists $T_3 > 0$ such that, for any $\varepsilon > 0$ and $0 < T_2 < T_3$, all signals are bounded at time T_2 and $\|e_\alpha\| \le \varepsilon$ for any $t \in [T_2, T_3)$, where it has been proved that T_3 can be extended to be infinite. Hence, the subsequent analysis considers the stability of the closed-loop system for $t \in [T_2, \infty)$.

From Eq. (29), the derivative of V_3 can be further written as

$$\dot{V}_3 \le -\mu_3\sqrt{V_3} + \gamma^2\varepsilon^2$$

where

$$\mu_3 = \min\{\mu_{31}, \mu_{32}, \mu_{33}, \mu_{34}\}$$

with

$$\begin{aligned}\mu_{31} &= \sqrt{2}\lambda_{\min}(K_2)\\ \mu_{32} &= \lambda_{\min}(K_4)\sqrt{2/\lambda_{\max}(M)}\\ \mu_{33} &= \sqrt{2/\lambda_{\max}(\Gamma^{-1})}\lambda_{\min}(K_6\Omega)/\lambda_{\max}(\Omega)\\ \mu_{34} &= \sqrt{2}\lambda_{\min}(k_{a_1})\end{aligned}$$

According to Definition 1 and lemma 3.6 in Ref. [23], the solution of the closed-loop system is PFS, and the trajectories are bounded in finite time as

$$\lim_{\varsigma_1\to\varsigma_{1,0}}(x_1, \tilde{x}_2, \tilde{\theta}, x_a) \in \left(\sqrt{V_3(t)} \le \frac{\gamma^2\varepsilon^2}{(1-\varsigma_1)\mu_3}\right) \tag{B1}$$

where scalars $\varsigma_1, \varsigma_{1,0}$ satisfy $0 < \varsigma_1 \le 1$ and $0 < \varsigma_{1,0} < 1$. The settling time to reach Eq. (B1) can be given by

$$T_1^* \le T_2 + \frac{2\sqrt{V_3(T_2)}}{\mu_3\varsigma_{1,0}}$$

where $V_3(T_2)$ is the value of V_3 at T_2. Furthermore, it follows from Eq. (16) that x_2 is also bounded.

The preceding analysis takes the input saturation into account. In another case, there does not exist input saturation. Consider the following candidate Lyapunov function:

$$V_4 = V_2 + \frac{1}{2}\tilde{x}_2^T M \tilde{x}_2 + \frac{1}{2}\tilde{\theta}^T \Gamma^{-1}\tilde{\theta}$$

Using the same calculation as V_3, and invoking $\Delta F = 0$ and $\dot{x}_a = 0$, it follows that

$$\begin{aligned}\dot{V}_4 \le & -x_1^T \Lambda K_1 \Lambda^T x_1 - x_1^T K_2 \frac{x_1}{\|x_1\|} - \left(\lambda_{\min}(K_3) - \frac{1}{2}\right)\|\tilde{x}_2\|^2 \\ & - \tilde{x}_2^T K_4 \frac{\tilde{x}_2}{\|\tilde{x}_2\|} k - \tilde{\theta}^T \frac{K_6 \Omega \tilde{\theta}}{\|\Omega\tilde{\theta}\|} + \frac{1}{2}\|K_5\|^2 \|x_a\|^2 \\ & + \gamma^2 e_\alpha^T e_\alpha - \gamma^2 \left\| e_\alpha - \frac{1}{2\gamma^2}\Lambda^T x_1 \right\|^2\end{aligned}$$

Noting $\|x_a\| < \eta$ and the inequalities in Eq. (28), we have

$$\begin{aligned}\dot{V}_4 \le & -\lambda_{\min}(K_2)\|x_1\| - \lambda_{\min}(K_4)\|x_2\| - \lambda_{\min}(K_6\Omega)/\lambda_{\max}(\Omega)\|\tilde{\theta}\| \\ & + \frac{1}{2}\eta^2\|K_5\|^2 + \gamma^2\varepsilon^2 \le -\mu_4\sqrt{V_4} + \varepsilon^*\end{aligned}$$

where $\varepsilon^* = (1/2)\eta^2\lambda_{\max}^2(K_5) + \gamma^2\varepsilon^2$; and $\mu_4 = \min\{\mu_{41}, \mu_{42}, \mu_{43}\}$ with $\mu_{41} = \mu_{31}$, $\mu_{42} = \mu_{32}$, and $\mu_{43} = \mu_{33}$.

Hence, the signals of the closed-loop system are bounded by

$$\lim_{\varsigma_2 \to \varsigma_{2,0}} (x_1, \tilde{x}_2, \tilde{\theta}) \in \left(\sqrt{V_4(t)} \le \frac{\varepsilon^*}{(1-\varsigma_2)\mu_4} \right) \tag{B2}$$

in finite time:

$$T_2^* \le T_2 + \frac{2\sqrt{V_4(T_2)}}{\mu_4 \varsigma_{2,0}}$$

where scalars $\varsigma_2, \varsigma_{2,0}$ satisfy $0 < \varsigma_2 \le 1$ and $0 < \varsigma_{2,0} < 1$, and $V_4(T_2)$ is the value of V_4 at T_2. Then, x_2 is bounded from Eq. (16).

Therefore, from the preceding analysis, it can be summarized that, whether input saturation exists or not, the closed-loop system is PFS, and the tracking errors x_1 and x_2 as well as the estimation error $\tilde{\theta}$ converge in finite time: $T^* = \max\{T_1^*, T_2^*\}$. This completes the proof.

Acknowledgment

This work is supported by the Major Program of National Natural Science Foundation of China under grant numbers 61690210 and 61690212.

References

[1] Huang, P., Wang, M., Meng, Z., Zhang, F., Liu, Z., and Chang, H., "Reconfigurable Spacecraft Attitude Takeover Control in Post-Capture of Target by Space Manipulators," *Journal of the Franklin Institute*, Vol. 353, No. 9, 2016, pp. 1985–2008. https://doi.org/10.1016/j.jfranklin.2016.03.011

[2] Huang, P., Lu, Y., Wang, M., Meng, Z., Zhang, Y., and Zhang, F., "Postcapture Attitude Takeover Control of a Partially Failed Spacecraft with Parametric Uncertainties," *IEEE Transactions on Automation Science and Engineering*, Vol. 16, No. 2, 2019, pp. 919–930. https://doi.org/10.1109/TASE.8856

[3] Bergmann, E., and Dzielski, J., "Spacecraft Mass Property Identification with Torque-Generating Control," *Journal of Guidance, Control, and Dynamics*, Vol. 13, No. 1, 1990, pp. 99–103. https://doi.org/10.2514/3.20522

[4] Wilson, E., Lages, C., and Mah, R., "On-Line, Gyro-Based, Mass-Property Identification for Thruster-Controlled Spacecraft Using Recursive Least Squares," *45th IEEE International Midwest Symposium on Circuits and Systems*, Vol. 2, IEEE, New York, 2002, pp. 334–337. https://doi.org/10.1109/MWSCAS.2002.1186866

[5] Ma, O., Dang, H., and Pham, K., "On-Orbit Identification of Inertia Properties of Spacecraft Using a Robotic Arm," *Journal of Guidance, Control, and Dynamics*, Vol. 31, No. 6, 2008, pp. 1761–1771. https://doi.org/10.2514/1.35188

[6] Norman, M. C., and Peck, M. A., "In-Orbit Estimation of Inertia and Momentum-Actuator Alignment Parameters," *Journal of Guidance, Control, and Dynamics*, Vol. 34, No. 6, 2011, pp. 1798–1814. https://doi.org/10.2514/1.53692

[7] Ahmed, J., Coppola, V. T., and Bernstein, D. S., "Adaptive Asymptotic Tracking of Spacecraft Attitude Motion with Inertia Matrix Identification," *Journal of Guidance, Control, and Dynamics*, Vol. 21, No. 5, 1998, pp. 684–691. https://doi.org/10.2514/2.4310

[8] Filipe, N., and Tsiotras, P., "Adaptive Position and Attitude-Tracking Controller for Satellite Proximity Operations Using Dual Quaternions," *Journal of Guidance, Control, and Dynamics*, Vol. 38, No. 4, 2015, pp. 566–577. https://doi.org/10.2514/1.G000054

[9] Zhao, Q., and Duan, G., "Adaptive Finite-Time Tracking Control of 6-DOF Spacecraft Motion with Inertia Parameter Identification," *IET Control Theory and Applications*, Vol. 13, No. 13, 2019, pp. 2075–2085. https://doi.org/10.1049/iet-cta.2019.0245

[10] Nuthi, P., and Subbarao, K., "Computational Adaptive Optimal Control of Spacecraft Attitude Dynamics with Inertia-Matrix Identification," *Journal of Guidance, Control, and Dynamics*, Vol. 40, No. 5, 2017, pp. 1258–1262. https://doi.org/10.2514/1.G000706

[11] Chowdhary, G., and Johnson, E., "Theory and Flight Test Validation of Long Term Learning Adaptive Flight Controller," *AIAA Guidance, Navigation, and Control Conference*, AIAA Paper 2008-6781, 2008. https://doi.org/10.2514/6.2008-6781

[12] Chowdhary, G., and Johnson, E., "Concurrent Learning for Convergence in Adaptive Control Without Persistency of Excitation," *49th IEEE Conference on Decision and Control (CDC)*, IEEE, New York, 2010, pp. 3674–3679. https://doi.org/10.1109/CDC.2010.5717148

[13] Valverde, A., and Tsiotras, P., "Spacecraft Trajectory Tracking with Identification of Mass Properties Using Dual Quaternions," *AIAA Guidance, Navigation, and Control Conference*, AIAA Paper 2018-1576, 2018. https://doi.org/10.2514/6.2018-1576

[14] Xiao, B., Hu, Q., Zhang, Y., and Huo, X., "Fault-Tolerant Tracking Control of Spacecraft with Attitude-Only Measurement Under Actuator Failures," *Journal of Guidance, Control, and Dynamics*, Vol. 37, No. 3, 2014, pp. 838–849. https://doi.org/10.2514/1.61369

[15] Sun, L., and Huo, W., "Robust Adaptive Relative Position Tracking and Attitude Synchronization for Spacecraft Rendezvous," *Aerospace Science and Technology*, Vol. 41, Feb. 2015, pp. 28–35. https://doi.org/10.1016/j.ast.2014.11.013

[16] Huang, Y., and Jia, Y., "Robust Adaptive Fixed-Time Tracking Control of 6-DOF Spacecraft Fly-Around Mission for Noncooperative Target," *International Journal of Robust and Nonlinear Control*, Vol. 28, No. 6, 2018, pp. 2598–2618. https://doi.org/10.1002/rnc.4038

[17] Kristiansen, R., Grøtli, E. I., Nicklasson, P. J., and Gravdahl, J. T., "A Model of Relative Translation and Rotation in Leader-Follower Spacecraft Formations," *Modeling, Identification and Control*, Vol. 28, No. 1, 2007, pp. 3–14. https://doi.org/10.4173/mic.2007.1.1

[18] Kristiansen, R., Nicklasson, P. J., and Gravdahl, J. T., "Spacecraft Coordination Control in 6-DOF: Integrator Backstepping vs Passivity-Based Control," *Automatica*, Vol. 44, No. 11, 2008, pp. 2896–2901. https://doi.org/10.1016/j.automatica.2008.04.019

[19] Zhang, F., and Duan, G. R., "Robust Adaptive Integrated Translation and Rotation Finite-Time Control of a Rigid Spacecraft with Actuator Misalignment and Unknown Mass Property," *International Journal of Systems Science*, Vol. 45, No. 5, 2012, pp. 1007–1034. https://doi.org/10.1080/00207721.2012.743618

[20] Xu, Y., Tatasch, A., and Fitz-Coy, N., "Chattering Free Sliding M ode Control for a 6 DOF Formation Flying Mission," *AIAA Guidance, Navigation, and Control Conference*, AIAA Paper 2005-6464, 2005. https://doi.org/10.2514/6.2005-6464

[21] Wang, M., Luo, J., Yuan, J., and Walter, U., "An Integrated Control Scheme for Space Robot After Capturing Non-Cooperative Target,"

Acta Astronautica, Vol. 147, June 2018, pp. 350–363. https://doi.org/10.1016/j.actaastro.2018.04.016

[22] Zhou, B. Z., Cai, G. P., Liu, Y. M., and Liu, P., "Motion Prediction of a Non-Cooperative Space Target," *Advances in Space Research*, Vol. 61, No. 1, 2018, pp. 207–222. https://doi.org/10.1016/j.asr.2017.10.028

[23] Zhu, Z., Xia, Y., and Fu, M., "Attitude Stabilization of Rigid Spacecraft with Finite-Time Convergence," *International Journal of Robust and Nonlinear Control*, Vol. 21, No. 6, 2011, pp. 686–702. https://doi.org/10.1002/rnc.v21.6

[24] Chowdhary, G., and Johnson, E., "A Singular Value Maximizing Data Recording Algorithm for Concurrent Learning," *American Control Conference*, IEEE, New York, 2011, pp. 3547–3552. https://doi.org/10.1109/ACC.2011.5991481

[25] Tsiotras, P., and Valverde, A., "Dual Quaternions as a Tool for Modeling, Control, and Estimation for Spacecraft Robotic Servicing Missions," *Journal of the Astronautical Sciences*, July 2019. https://doi.org/10.1007/s40295-019-00181-4

[26] Yoo, D. S., and Chung, M. J., "A Variable Structure Control with Simple Adaptation Laws for Upper Bounds on the Norm of the Uncertainties," *IEEE Transactions on Automatic Control*, Vol. 37, No. 6, 1992, pp. 860–865. https://doi.org/10.1109/9.256348

[27] Bhat, S. P., and Bernstein, D. S., "Continuous Finite-Time Stabilization of the Translational and Rotational Double Integrators," *IEEE Transactions on Automatic Control*, Vol. 43, No. 5, 1998, pp. 678–682. https://doi.org/10.1109/9.668834

[28] Dong, W., Farrell, J. A., Polycarpou, M. M., Djapic, V., and Sharma, M., "Command Filtered Adaptive Backstepping," *IEEE Transactions on Control Systems Technology*, Vol. 20, No. 3, 2012, pp. 566–580. https://doi.org/10.1109/TCST.2011.2121907